α-D-Glucopyranosyl-(1→2)-[6-*O*-(L-tryptophanyl)-β-D-fructofuranoside]

Kwaku Kyeremeh [1,*] , **Samuel Kwain** [1], **Gilbert Mawuli Tetevi** [1], **Anil Sazak Camas** [2], **Mustafa Camas** [2] , **Aboagye Kwarteng Dofuor** [3], **Hai Deng** [4] **and Marcel Jaspars** [4]

[1] Marine and Plant Research Laboratory of Ghana, Department of Chemistry, School of Physical and Mathematical Sciences, University of Ghana, P.O. Box LG 56, Legon-Accra, Ghana; kwainsamuel75@gmail.com (S.K.); gilberttet@gmail.com (G.M.T.)

[2] Department of Bioengineering, Munzur University, 62000 Tunceli, Turkey; anilsazak@gmail.com (A.S.C.); mustafacamas@gmail.com (M.C.)

[3] Department of Biochemistry, Cell and Molecular Biology, University of Ghana, P. O. Box LG 54 Legon-Accra, Ghana; akdofuor@st.ug.edu.gh

[4] Marine Biodiscovery Centre, Department of Chemistry, University of Aberdeen, Old Aberdeen, AB24 3UE Scotland, UK; h.deng@abdn.ac.uk (H.D.); m.jaspars@abdn.ac.uk (M.J.)

[*] Correspondence: kkyeremeh@ug.edu.gh; Tel.: +2-3320-789-1320

check for updates

Abstract: The *Mycobacterium* sp. BRS2A-AR2 is an endophyte of the mangrove plant *Rhizophora racemosa* G. Mey., which grows along the banks of the River Butre, in the Western Region of Ghana. Chemical profiling using ^{1}H-NMR and HRESI-LC-MS of fermentation extracts produced by the strain led to the isolation of the new compound, α-D-Glucopyranosyl-(1→2)-[6-*O*-(L-tryptophanyl)-β-D–fructofuranoside] or simply tortomycoglycoside (**1**). Compound **1** is an aminoglycoside consisting of a tryptophan moiety esterified to a disaccharide made up of β-D-fructofuranose and α-D-glucopyranose sugars. The full structure of **1** was determined using UV, IR, 1D, 2D-NMR and HRESI-LC-MS data. When tested against *Trypanosoma brucei* subsp. *brucei*, the parasite responsible for Human African Trypanosomiasis in sub-Saharan Africa, **1** (IC_{50} 11.25 μM) was just as effective as *Coptis japonica* (Thunb.) Makino. (IC_{50} 8.20 μM). The extract of *Coptis japonica* (Thunb.) Makino. is routinely used as laboratory standard due to its powerful antitrypanosomal activity. It is possible that, compound **1** interferes with the normal uptake and metabolism of tryptophan in the *T. brucei* subsp. *brucei* parasite.

Keywords: endophytes; mangroves; glycosides; trypanosomes; antiparasitics

1. Introduction

Carbohydrate-based natural products constitute a very potent group of compounds with promising prospects as future drugs [1]. Currently, there are many carbohydrate natural product derived compounds that are already drugs and these include: The polysaccharides, tragacanth (diarrhea and constipation) [2], astragalus (cancer) [3], lentinan (cancer and hepatitis B) [4], tremella (cancer and chronic bronchitis) [5,6], icodextrin (peritoneal dialysis) [7] and pentosan polysulfate (interstitial cystitis) [8]; the oligosaccharides, lactulose (constipation and hepatic encephalopathy) [9], sucralfate (active duodenal ulcers) [10]; and the monosaccharides, miglitol (anti-diabetic) [11] and meglumine (excipient) [12].

Glycosylated natural products are defined as natural compounds where the carbohydrate part (glycone), either monomers or oligomers of different structures, is covalently bound to another chemical structure (aglycone). The aglycone encompasses natural product scaffolds such as terpenes, steroids, alkaloids, ribosomal and non-ribosomal peptides, modified amino acids, polyketides, macrolides, flavonoids, polyenes, coumarins, anthracyclines, iridoids and lignans [13–16]. Glycosides display

very broad bioactivities because, part of their structures are composed of one or more stereocenter laden sugar portions with numerous hydroxyls and other functionalities that confer increased drug water solubility, increased bioavailability, decreased toxicity, effective drug targeting, bioactivity, strong molecular targeting and organism specificity while the non-sugar portion or aglycones, represent molecules that also have many bioactivities [17]. Glycosides have been shown to exhibit potent α- and β-glucosidase inhibition (nojirimycin and acarbose) [18–20], antibacterial (streptomycin, erythromycin A, vancomycin, gentamycin, amikacin, kanamycin, neomycin and bleomycin) [21–23], anticancer (digoxin and biselyngbyaside) [24,25], antifungal (hassallidin A and B, and macrolide CE-108) [26–28], antiparasitic (amphotericin B and paromomycin) [29–32] and antioxidant (floridoside) activities [33]. Biologically, carbohydrates are known to participate in energy storage and constitute a major component of structural polymers in microbes, plants and invertebrates [34–37]. Furthermore, as a result of their structural and chemical characteristics, they play many other key biological roles such as fertilization signaling, pathogen recognition, cellular interactions and tumor metastasis [38–41]. Therefore, it may be proposed that naturally occurring glycosides constitute a possible source of future antiparasitic, antitumor, antiviral, anticoagulant, antioxidant and anti-inflammatory drugs.

In the last four years, we have collected several mangrove plants including *Conocarpus erectus* Linn., *Laguncularia racemosa* (L.) C.F. Gaertn. and *Rhizophora racemosa* G. Mey. from unexplored unique and extreme environments in the Ghanaian Western, Volta, and Brong Ahafo Regional wetlands. From these samples, we have isolated many cultivable strains of endophytic microbes (e.g., *Penicillium herquei* strain BRS2A-AR, *Cladosporium oxysporum* strain BRS2A-AR2F, etc.) from the different plant parts that in turn produce culture extracts, which show antiparasitic activity against the neglected tropical parasites *Trypanosoma brucei* subsp. *brucei* strain 927/4 GUTat10.1, *Leishmania donovani* (Laveran and Mesnil) Ross, *Leishmania major* (Yakimoff and Schokhor), *Schistosoma mansoni* (Sambon) and *Trichomonas mobilensis* (U.S.A.: M776 [M776]). Among these mangrove endophytic strains was the *Mycobacterium* sp. BRS2A-AR2 (GenBank ID: KT945161), isolated from the aerial roots of the Ghanaian mangrove plant, *R. racemosa*. We have previously reported for the first time ever that, strain BRS2A-AR2 biosynthesizes gold nanoparticles that are cytotoxic to HUVEC and HeLa cell lines [42].

The mangrove plant *Rhizophora racemosa* G. Mey. is a multi-stemmed rambling to columnar stilt-rooted mangrove tree that grow up to about 30 m (100 ft.) tall but, appear to be shorter, more branched and scrubby in marginal habitats [43,44]. The leaves are opposite, simple, bright green, leathery, obovate, with generally curved surface, obtuse blunt apex with a minute lip folded under [45]. The lower surfaces of the leaves have evenly scattered tiny corky warts, which appear as black spots on dried leaves. The flowers show flat, slightly hairy petals, which are stiff erect with non-reflexed calyx lobes [46]. They have thick, short rounded bracteoles and rounded flower buds. The stem of the axillary flowers branches up to six times, making a maximum cluster size of 128 [43,46].

The *Mycobacteria* are members of the *Actinobacteria* with characteristic rod-shapes and are mostly gram-positive aerobes or facultative anaerobes. This genus includes pathogens known to cause serious diseases in mammals (Table S1). The strain *Mycobacterium* sp. BRS2A-AR2 colonies used in the present study were aerobic, gram reaction positive, yellowish orange, viscous and non-spore forming in an ISP2 agar medium. According to a phylogenetic analysis based on 16S rRNA gene sequencing, BRS2A-AR2 formed a distinct branch from other *Mycobacterium* species, notably from its nearest neighbors, making it a new species [42]. The closest relatives of strain BRS2A-AR2 were *Mycobacterium houstonense* ATCC 49403T (99.1%; 12 nt differences at 1440 locations), *Mycobacterium senegalense* AY457081T (99.1%; 12 nt differences at 1440 locations) and *Mycobacterium pallens* czh-8T Dq370008 (98.81%; 17 nt differences at 1434 locations). *Mycobacterium houstonense* is a non-tuberculous species rarely responsible for human infection [47] and similarly for *Mycobacterium pallens* [48]. On the other hand, *Mycobacterium senegalense* is responsible for Bovine farcy, which is a chronic suppurative granulomatous inflammation of the skin and lymphatics of cattle and is seen mostly in sub-Saharan Africa [49]. We have not performed any clinical microbiology tests to prove the pathogenicity of strain BRS2A-AR2 or otherwise. However, BRS2A-AR2 has not been previously isolated from any diseased human or animal and given that the

strain is an endophyte of a mangrove plant that produced a very distinct 16S rRNA gene sequence, it has been safe to work with it so far.

Large scale culture of *Mycobacterium* sp. BRS2A-AR2 in ISP2 fermentation media at pH 5.0, 28 °C and 220 rpm produced extracts which upon solvent partitioning by a modification of Kupchan's method gave four fractions hexane (FH), dichloromethane (FD), methanol/water (FM) and butanol/water (WB). Phytochemical screening on thin-layer chromatography (TLC) plates using iodine tank, Dragendorff, phosphomolybdic acid, antimony (III) chloride and Ninhydrin reagents showed the WB to contain the most interesting metabolites. The fraction WB was therefore subjected to a Sephadex LH-20 size exclusion chromatography to give four fractions of which WB-SF4 was found to contain the compound of interest. HPLC of WB-SF4 led to the isolation of the potent glycoside antitrypanosomal compound (Figure 1), α-ᴅ-glucopyranosyl-(1→2)-[6-*O*-(ʟ-tryptophanyl)-β-ᴅ–fructofuranoside] or simply tortomycoglycoside (**1**) (2.3 mg/L). The structure of this new compound was determined using a combination of 1D- and 2D-NMR techniques with high-resolution liquid chromatography tandem mass spectrometry (HRESI-LC-MS) data and TLCs.
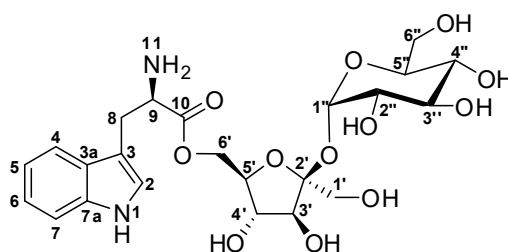
Figure 1. Structure of α-ᴅ-Glucopyranosyl-(1→2)-[6-*O*-(ʟ-tryptophanyl)-β-ᴅ-fructofuranoside] (**1**).

2. Results

The compound **1** was obtained at t_R of 20 min on reverse phase HPLC. Compound **1** is a light yellow pungent oil when completely free of solvent. The HRESI-LC-MS of compound **1** gave *m/z* 529.2630 corresponding to molecular formula of $C_{23}H_{33}N_2O_{12}^+$ (Δ = +0.06 ppm and 9 degrees of unsaturation) for $[M + H]^+$. An $[M + Na]^+$ ion was also seen at *m/z* 551.2449 corresponding to the molecular formula $C_{23}H_{32}N_2NaO_{12}^+$ (Δ = +0.06 and 9 degrees of unsaturation), which further and undoubtedly confirmed the mass of this new compound under electrospray ionization conditions (Figure S2). Due to the presence of the many hydroxyl groups, compound **1** showed a prominent [M + H − OH]$^+$ at 511.2527 as the base peak indicating random facile loss of H_2O from different parts of the molecule. Compound **1** is an amino acid *O*-glycoside that belongs to the group of compounds known as the glycoconjugates. Analysis of the ^1H, ^{13}C and multiplicity edited Pulsed Field Gradient Heteronuclear Single Quantum Coherence (gHSQCAD) spectrum of **1**, suggested the presence of five quaternaries, 14 methine and four methylene carbons with no methyl groups. The ^1H-NMR chemical shifts δ_H 10.9 (1H, d, *J* = 2.9 Hz, NH-1), 7.22 (1H, d, *J* = 2.9 Hz, H-2), 7.59 (1H, d, *J* = 8.1 Hz, H-4), 6.97 (1H, ddd, *J* = 8.1, 7.0, 1.2 Hz, H-5), 7.06 (1H, m, H-6), 7.35 (1H, m, H-7), 3.02 (2H, dd, *J* = 15.3, 8.7 Hz, H₂-8), 3.55 (1H, m, H-9) and 3.59 (2H, d, *J* = 2.3, 4.3 Hz, NH-9) together with the δ_C 124.2 (C-2), 109.1 (C-3), 127.2 (C-3a), 118.3 (C-4), 118.4 (C-5), 120.9 (C-6), 111.4 (C-7), 136.3 (C-7a), 26.9 (C-8), 54.5 (C-9) and 170.8 (C-10) provided direct evidence for the presence of the aromatic tryptophan residue. Detailed analysis of the ^1H-^1H Homonuclear Correlation Spectroscopy (gCOSY) spectrum showed correlations H-2/NH-1, H-4/H-5, H-6/H-7 and H-8/H-9, which were further supported by similar ^1H-^1H Total Correlation Spectroscopy (2D-TOCSY) correlations, including H-2/NH-1, H-4/H-7, H-5/H-6, H-6/H-4, H-7/H-4 and H-8/H-9 to further confirm the presence of a tryptophan moiety. Several Pulsed Field Gradient ^1H-^{13}C Heteronuclear Multiple Bond Correlations (gHMBCAD) providing connections between the isolated spin-systems of the aromatic tryptophan through quaternaries and heteroatoms were observed and include C-2, C-3, C-3a, C-9 and C-10 to H2-8, C-3, C-3a, C-6 and C-7a

to H-4, C-2, C-3, C-3a and C-7a to 1NH, C-3, C-3a and C-7a to H-2, C-3a, C-4 and C-5 to H-7, C-3a and C-7 to H-5 and finally C-4, C-5 and C-7a to H-6.

In the ^{13}C NMR spectrum, the presence of several peaks between 65–95 ppm suggested the presence of sugar moieties in compound (**1**). The gHMBCAD correlations C-10 to H-5′ and H-6′ and the chemical shifts of C-10 and C-6′′ provided direct proof of attachment of the tryptophan residue to a sugar through an ester bond. The identities of the sugars were found to be β-ᴅ-fructofuranose and α-ᴅ-glucopyranose after inspection of the chemical shifts, anomeric coupling constants, ^{1}H-^{1}H Rotating-frame Overhauser Spectroscopy (ROESY) data, molecular modeled structure and chiral TLCs. The β-ᴅ-fructofuranose ring had δ$_C$ 62.2 (C-1′), 104.0 (C-2′), 77.2 (C-3′), 74.3 (C-4′), 82.5 (C-5′) and 62.1 (C-6′) corresponding to δ$_H$ 3.41 (2H, d, J = 3.1 Hz, H-1′), 3.89 (1H, d, J = 8.3 Hz, H-3′), 3.79 (1H, t, J = 7.7 Hz, H-4′), 3.57 (1H, dt, J = 7.7, 2.2 Hz, H-5′) and 3.41 (2H, d, J = 2.3 Hz, H-6′), respectively. The gCOSY correlation H-5′/H-4′ along with the 2D-TOCSY correlations H-4′/H-3′, H-5′/H-3′, H-5′/H-4′, H-6′/H-3′ and H-6′/H-4′ confirmed the continuous spin system of the β-ᴅ-fructofuranose residue while the gHMBCAD correlations C-4′ to H-3′, C-5′ to H-3′, C-5′ to H-4′, C-1′ to H-3′ and C-6′ to H-4′ showed the positions of quaternaries and heteroatoms in the ring. The gHMBCAD correlation C-2′ to H-1′′ helped to solve the rest of the structure, which was shown to be an α-ᴅ-glucopyranose ring after similar examination of the sugar ring, which is explained above. The α-ᴅ-glucopyranose ring carbon chemical shifts were δ$_C$ 91.8 (C-1′′), 71.7 (C-2′′), 72.8 (C-3′′), 69.9(C-4′′), 72.9 (C-5′′) and 60.5 (C-6′′) and δ$_H$ 5.19 (1H, d, J = 4.1 Hz, H-1′′), 3.20 (1H, dd, J = 9.7, 3.9 Hz, H-2′′), 3.49 (1H, t, J = 9.3 Hz, H-3′′), 3.14 (1H, t, J = 9.4 Hz, H-4′′), 3.65 (1H, ddd, J = 9.7, 4.7, 2.4 Hz, H-5′′), 3.52 (1H, dd, J = 10.0, 4.8 Hz, H-6′′) and 3.50 (1H, dd, J = 10.0, 2.6 Hz, H-6′′), respectively. The gCOSY correlations H-2′′/H-1′′, H-4′′/H-5′′ and H-4′′/H-3′′ supported by many 2D-TOCSY correlations that include H-1′′/H-3′′, H-1′′/H-2′′, H-4′′/H-5′′, H-2′′/H-5′′, H-4′′/H-6′′, H-2′′/H-3′′, H-4′′/H-2′′, H-5′′/H-2′′, H-2′′/H-4′′, H-5′′/H-4′′, H-3′′/H-4′′, H-6′′/H-5′′, H-6′′/H-4′′, H-4′′/H-1′′, H-2′′/H-1′′, H-5′′/H-1′′ and gHMBCAD correlations C-5′′ to H-1′′, C-4′′ to H-3′′, C-5′′ to H-4′′, C-2′′ to H-3′′ and C-6′′ to H-4′′ provided proof of structure for the α-ᴅ-glucopyranose ring moiety in compound (**1**). The absence of correlations in the ^{1}H-^{1}H ROESY data, indirectly confirms the disposition of the protons in both the β-ᴅ-fructofuranose and α-ᴅ-glucopyranose rings.

Complete NMR data for Compound **1** is given in Table 1 while the raw data can be found in the Supplementary Figures S4–12. In Figures 2–4, a visual representation of COSY, HMBC, 2D-TOCSY and ROESY correlations are shown.
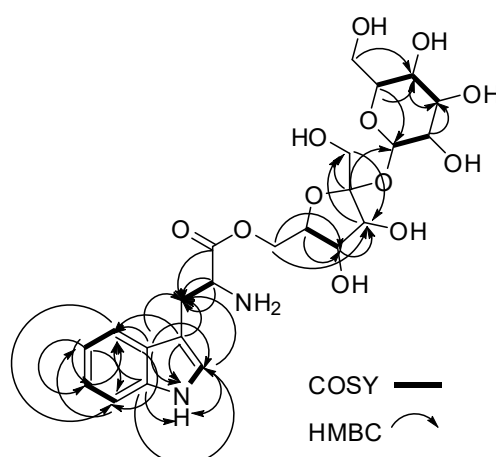
Figure 2. Key COSY (bold lines) and ^{13}C-^{1}H HMBC (single arrows) correlations for compound **1**.

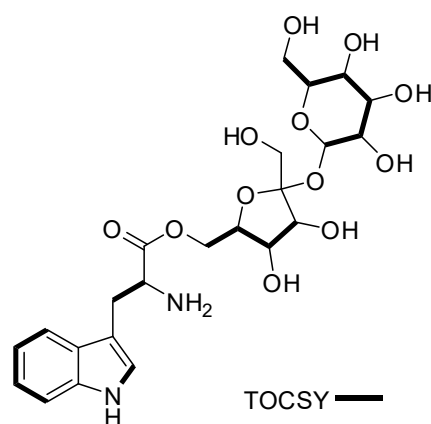**Figure 3.** Key TOCSY (bold lines) correlations for compound **1**.
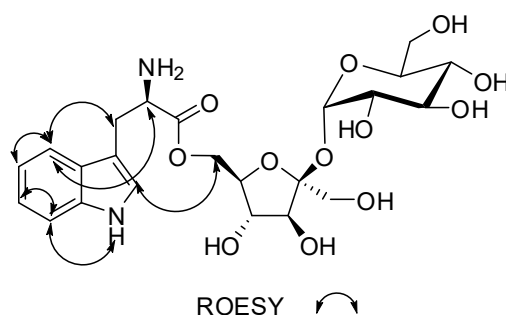

Figure 4. Key ROESY (double arrow) correlations for compound **1**.

Table 1. 1D and 2D-NMR spectroscopic data for compound (**1**) in DMSO-d_6, in ppm.

#	δc mult	δH mult (J Hz)	¹H-¹H COSY	HMBC	TOCSY
1 NH		10.9, d (2.9)	2	C-2, C-3, C-3a, C-7a	
2	124.2, CH	7.22, d (2.9)	1NH	C-3, C-3a, C-7a	1NH
3	109.1, C				
3a	127.2, C				
4	118.3, CH	7.59, d (8.1)	5	C-3, C-3a, C-6, C-7a	5, 6,7
5	118.4, CH	6.97, m	4	C-3a, C-7	4, 6, 7
6	120.9, CH	7.06, m	7	C-4, C-5, C-7a	4, 5, 7
7	111.4, CH	7.35, m	6	C-3a, C-4, C-5	4, 5, 6
7a	136.3, C				
8	26.9, CH₂	3.02, dd (15.3, 8.7)	8, 9	C-2, C-3, C-3a, C-9, C-10	9, 2
		3.32, dd (15.1, 4.4)	8, 9		
9	54.5, CH	3.55, m	8		8
9 NH₂		3.59, dd (2.3, 4.3)			
10	170.8, C				
1′	62.2, CH₂	3.41, d (3.1)		C-2′, C-3′	3′, 4′, 6′
2′	104.0, C				
3′	77.2, CH	3.89, d (8.1)		C-1′, C-4′, C-6′	4′, 5′
4′	74.3, CH	3.79, t (7.7)	5′	C-1′, C-5′, C-6′	3′, 5′
5′	82.5, CH	3.57, dt (7.7, 2.2)	4′		3′, 4′
6′	62.1, CH₂	3.41, d (2.3)		C-10	1′, 3′, 4′
1″	91.8, CH	5.19, d (4.1)	2″	C-5″, C-2′	5″, 2″,
2″	71.7, CH	3.20, dd (9.7, 3.9)	1″		5″, 3″, 4″, 1″
3″	72.8, CH	3.49, t (9.7)	4″	C-2″, C-4″	5″, 2″, 4″, 1″
4″	69.9, CH	3.14, t (9.5)	3″, 5″	C-5″, C-6″	5″, 6″, 2″, 1″
5″	72.9, CH	3.65, ddd (9.7, 4.7, 2.4)	4″		1″, 2″, 3″, 4″
6″	60.5, CH₂	3.52, dd (10, 4.8,)			5″, 4″
		3.50, dd (10, 2.6)			

Compound **1** showed very interesting and consistent results when tested against our laboratory strain of *T. brucei brucei*. The IC$_{50}$ value of 11.25 µM calculated for **1** was almost as effective as that

of the routine laboratory standard *Coptis japonica* (IC$_{50}$ 8.20 μM). Detailed examination of the dose response curve for **1** (Figure 5) showed the potential for this compound to be significantly lethal and potent against *T. brucei brucei* cells.
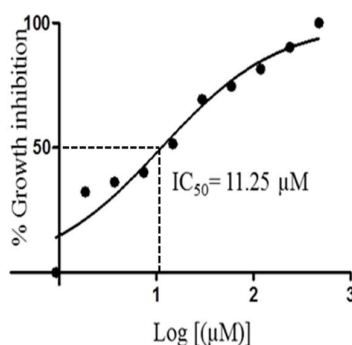
Figure 5. IC$_{50}$ curve for compound **1** when tested against *Trypanosoma brucei brucei*.

It is possible that, compound **1** described herein can affect the easy recognition of the amino acid tryptophan within the extracellular matrix. Therefore, subsequent uptake of tryptophan, metabolism of tryptophan and the incorporation of tryptophan into important enzymes such as proteases and phospholipases that contribute to the normal functions of the *T. brucei brucei* parasite is perturbed [50,51].

3. Experimental Section

3.1. General Experimental Procedures

1D and 2D NMR data were recorded on a Bruker AVANCE III HD Prodigy (BRUKER, Sylvenstein, Germany) at 500 and 125 MHz for ^{1}H and ^{13}C, respectively. This instrument was optimized for ^{1}H observation with pulsing/decoupling of ^{13}C and ^{15}N, with 2H lock channels equipped with shielded z-gradients and cooled preamplifiers for ^{1}H and ^{13}C. The ^{1}H and ^{13}C chemical shifts were referenced to the solvent signals (δ_H 2.50 (1H, p) and δ_C 39.52 ppm in DMSO-d_6). High-resolution mass spectrometry data were measured using a ThermoScientific LTQXL-Discovery Orbitrap (Thermo Scientific, Bremen, Germany) coupled to an Accela UPLC-DAD system. The following conditions were used for mass spectrometric analysis: Capillary voltage 45 V, capillary temperature 320 °C, auxiliary gas flow rate 10–20 arbitrary units, sheath gas flow rate 40–50 arbitrary units, spray voltage 4.5 kV and mass range 100–2000 amu (maximum resolution 30,000). The ion source was normal electrospray ionization that acts both in positive and negative modes. Semi-preparative HPLC purifications were carried out using a Phenomenex Luna reverse-phase (C18 250 × 10 mm, L × i.d.) column connected to a Waters 1525 Binary HPLC pump Chromatograph with a 2998 photodiode array detector (PDA), column heater and in-line degasser. Detection was achieved on-line through a scan of wavelengths from 200 to 400 nm. This system was also used to record the UV profile for the compounds. IR was measured using a PerkinElmer FT-IR (UATR Two) spectrometer. All solvents were HPLC grade. Sephadex LH-20 and HP-20 resin were obtained from Sigma Aldrich (Munich, Germany).

3.2. Mangrove Plant Sample Collection

The Ghanaian mangrove plant *R. racemosa* was collected along the banks of the River Butre in the Western Region of Ghana at GPS coordinates: 4°49'43.73'N and 1°54'50.84'W elevation 7 m; eye altitude 437 m. The plant parts sampled were leaves, buds, submerged roots, aerial roots, aerial stems, fruit shoots and flowers.

3.3. Isolation and Purification of the Endophytic Mycobacterium Strain

Isolation, purification, identification and laboratory cultivation of the Ghanaian *Mycobacterium* sp. BRS2A-AR2 were previously described by us [42].

3.4. Fermentation

An Autoclaved Erlenmeyer flask (250 mL) plugged with non-absorbent cotton wool containing 50 mL of ISP2 (10 g of malt extract, 4 g each of yeast extract and D-glucose) fermentation media in distilled water with pH 5.0 was directly inoculated with spores of strain BRS2A-AR2 and incubated at 28 °C and 220 rpm for three days. This seed culture was subsequently used to inoculate nine autoclaved 1 L Erlenmeyer flasks, each containing 200 mL ISP2 media at pH 5.0 and plugged with non-absorbent cotton wool. The 1 L flasks were incubated at 28 °C and 220 rpm for 21 days. Two days before the culture incubation period was complete, autoclaved HP-20 resin was added at 50 g/L to each of the flasks under sterile conditions and the flasks were returned to the incubator.

3.4.1. Extraction and Purification

The *Mycobacterium* sp. strain BRS2A-AR2 fermentation broth (1.8 L) was filtered through a piece of glass wool under suction in a Buchner funnel to separate the supernatant from the mycelia. The supernatant was extracted with EtOAc and the mycelia and HP-20 resin were placed in a 1 L flask and extracted first with CH_2Cl_2 followed by MeOH. All extracts were combined and evaporated under reduced pressure to obtain a total crude extract (5.90 g). The total crude extract was subjected to a modification of Kupchan's solvent partitioning process [52] that gave the four fractions FH (1.2 g), FD (1.6 g), FM (0.50 g) and WB (2.3 g), with the compounds of interests concentrated in the FD and WB fractions. The Kupchan solvent partitioning process is able to simplify subsequent purification and isolation steps, chemical profiling and biological activity screening by separating the extract components according to their polarities. Briefly, the total crude extract was suspended in 200 mL of water and extracted three times over three consecutive days with CH_2Cl_2. The water layer was subsequently, extracted with *sec*-butanol once. The *sec*-butanol layer was dried under vacuum to give a butanol/water (WB) fraction and the remaining water layer discarded. The CH_2Cl_2 layer was dried under vacuum and suspended in 90/10 mixture of water/methanol. The 90/10 water/methanol mixture was extracted three times over three consecutive days with hexane. The hexane extract was dried under vacuum to give fraction hexane (FH). The 90/10 water/methanol layer was phase adjusted to 50/50 water/methanol and extracted three times with dichloromethane. The dichloromethane layer was dried under vacuum to give fraction dichloromethane (FD). Drying the 50/50 water/methanol layer under vacuum gives fraction methanol/water (FM). The fraction FH is the least polar fraction whilst WB is the most polar fraction. The WB fraction was then subjected to Sephadex LH-20 size exclusion chromatography by gravity to obtain four fractions that were labeled WB-SF1-4. Phytochemical screening with ninhydrin on TLC plates followed by ^{1}H-NMR showed the compound of interest to be concentrated in the WB-SF4 (0.34 g). Fraction WB-SF4 was therefore subjected to semi-preparative HPLC separation and purification using a Phenomenex Luna C18 column (C18 250 × 10 mm, L × i.d.). Gradients of Solvent A: H_2O (0.1% HCOOH) and Solvent B: CH_3CN (0.1% HCOOH; 100% A to 100% B in 30 min and hold for 30 min) were used as eluents with column flow rates set at 1.5 mL/min to afford compound **1** (2.5 mg, t_R = 20.0 min).

3.4.2. α-D-Glucopyranosyl-(1→2)-[6-*O*-(L-tryptophanyl)-β-D-fructofuranoside] (**1**)

Light yellow pungent oil; IR (neat) νmax 3482, 3040, 2922, 2853 and 1783 cm^{-1}; UV (H_2O:CH_3CN) λmax 238, 284 and 395 nm; for ^{1}H and ^{13}C NMR data, see Table 1; mass spectrometry data is detailed in Supplementary Figures S1 and S2.

3.4.3. Acid Hydrolysis of Compound **1**

Compound **1** (1.5 mg) was dissolved in MeOH (2 mL) and 5 N HCl (1 mL). The mixture was refluxed for 3 h. The solution was neutralized with NaOH, extracted with EtOAc and concentrated under vacuum. The sugars in the aqueous phase were identified as fructose and glucose by comparative TLC with standard sugars using the solvent system BuOH/EtOAc/2-propanol/HOAc/H_2O (7:20:12:7:6).

This acid hydrolysis further confirmed the identities of the two sugars present in the structure of compound **1**.

3.5. Bioassay Reagents

Fetal Bovine Serum (FBS), Roswell Park Memorial Institute (St. Louis, MO, USA); (RPMI) 1640, Iscove's Modified Dulbecco's Media IMDM, M-199, 2-[4-(2-hydroxyethyl)piperazin-1-yl]ethanesulfonic acid (HEPES), YI-S, adult bovine serum (ABS), gentamycin, penicillin-streptomycin-ʟ-glutamine (PSG), artesunate, alamar dye, dimethyl sulfoxide (DMSO), sodium citrate, adenine, sodium bicarbonate (NaHCO$_3$), AlbuMax II, sodium chloride (NaCl), potassium chloride (KCl), sodium phosphate dibasic (Na$_2$HPO$_4$), sodium phosphate monobasic (KH$_2$PO$_4$) and sodium hydroxide (NaOH), were purchased from Sigma-Aldrich, MO, USA. All other chemicals and reagents were of analytical grade.

3.5.1. Compound Preparation for Bioassay

A stock solution of compound **1** was prepared at a concentration of 100 mM. This was achieved by drying the compound with nitrogen gas and weighing on a balance (AND GH-120, A and D Company Limited, Tokyo, Japan) to ascertain the mass of the compound. Compound **1** was dissolved in an appropriate amount of DMSO to attain the desired concentration. The stock solution was vortexed (MSI Minishaker. IKA Company, Osaka, Japan) and filter sterilized into a vial through 0.45 μm millipore filters under sterile conditions and stored at −20 °C until use.

3.5.2. Cell Culture

The GUTat 3.1 strain of the bloodstream form of *T. brucei* parasites was used in this study. Parasites were cultured in vitro according to the conditions established previously by Yabu et al. in 1998 [53]. Parasites were used when they reached a confluent concentration of 1×10^6 parasites/mL. Estimation of parasitemia was done with the Neubauer counting chamber. Parasites were diluted to a concentration of 3×10^5 parasites/mL with an IMDM medium and used for the drug assay.

3.5.3. In Vitro Viability Test for Trypanosome Parasites

The Alamar Blue assay was carried out on treated and untreated trypanosome parasites to ascertain their viability. The assay was performed in a 96-well plate following the manufacturer's instructions, with modification. Briefly, 1.5×10^4 parasites were seeded with varied concentrations of the compound ranging from 0 to 100 μM. Final concentrations of DMSO were kept at 0.1%. After the incubation of parasites with or without the compound for 24 h at 37 °C in 5% CO$_2$, 10% Alamar Blue dye was added, and the parasites were incubated another 24 h in darkness. After a total of 48 h, the plate was read for absorbance at 540 nm using the Tecan Sunrise Wako spectrophotometer, AUSTRIA GmbH. The trend curve was drawn to obtain a 50% inhibitory concentration (IC$_{50}$) for the compound.

4. Conclusions

The Ghanaian *Mycobacterium* sp. BRS2A-AR2 (GenBank ID: KT945161) was previously isolated and characterized by our group from the aerial roots of the mangrove plant, *R. racemosa*. We also reported for the first time ever that, strain BRS2A-AR2 biosynthesizes gold nanoparticles that are cytotoxic to HUVEC and HeLa cell lines [42]. Herein we report that, the main metabolite produced in liquid culture by the strain BRS2A-AR2 is an amino acid glycoside (α-ᴅ-glucopyranosyl-(1→2)-[6-*O*-(ʟ-tryptophanyl)-β-ᴅ-fructofuranoside]) that consists of a tryptophan moiety esterified to a disaccharide made up of β-ᴅ-fructofuranose and α-ᴅ-glucopyranose rings. Compound **1**, exhibited potent antitrypanosomal effects when tested against the laboratory strain of *T. brucei brucei*. It is possible that, compound **1** interferes with the normal uptake and metabolism of tryptophan in the parasite.

Supplementary Materials: The following are available online http://www.mdpi.com/1422-8599/2019/2/M1066/s1.

Conflicts of Interest: The authors declare no conflicts of interests.

References

1. Zhang, Y.; Wang, F. Carbohydrate drugs: Current status and development prospect. *Drug Discov. Ther.* **2015**, *9*, 79–87. [CrossRef] [PubMed]

2. Upadhyay, R.K. Tulsi: A holy plant with high medicinal and therapeutic value. *IJGP* **2017**, *11*, S1–S12.

3. Wu, C.Y.; Ke, Y.; Zeng, Y.F.; Zhang, Y.W.; Yu, H.J. Anticancer activity of Astragalus polysaccharide in human non-small cell lung cancer cells. *Cancer Cell Int.* **2017**, *17*, 115. [CrossRef] [PubMed]

4. Ina, K.; Kataoka, T.; Ando, T. The use of lentinan for treating gastric cancer. *Anticancer Agents Med. Chem.* **2017**, *13*, 681–688. [CrossRef]

5. Jiang, R.Z.; Wang, Y.; Luo, H.M.; Cheng, Y.Q.; Chen, Y.H.; Gao, Y.; Gao, Q.P. Effect of the molecular mass of Tremella polysaccharides on accelerated recovery from cyclophosphamide-induced leucopenia in rats. *Molecules* **2012**, *17*, 3609–3617. [CrossRef] [PubMed]

6. Shi, X.; Wei, W.; Wang, N. Tremella polysaccharides inhibit cellular apoptosis and autophagy induced by Pseudomonas aeruginosa lipopolysaccharide in A549 cells through sirtuin 1 activation. *Oncol. Lett.* **2018**, *15*, 9609–9616. [PubMed]

7. Silver, S.A.; Harel, Z.; Perl, J. Practical considerations when prescribing icodextrin: A narrative review. *Am. J. Nephrol.* **2014**, *39*, 515–527. [CrossRef]

8. Kumagai, K.; Shirabe, S.; Miyata, N.; Murata, M.; Yamauchi, A.; Kataoka, Y.; Niwa, M. Sodium pentosan polysulfate resulted in cartilage improvement in knee osteoarthritis-An open clinical trial. *BMC Clin. Pharmacol.* **2010**, *10*, 7. [CrossRef]

9. Lee-Robichaud, H.; Thomas, K.; Morgan, J.; Nelson, R.L. Cochrane review: Lactulose versus polyethylene glycol for chronic constipation. *Evid. Based Child Health* **2011**, *6*, 824–864. [CrossRef]

10. Ulbrich, W.; Lamprecht, A. Targeted drug-delivery approaches by nanoparticulate carriers in the therapy of inflammatory diseases. *J. Royal Soc. Interface* **2009**, *7*, s55–S66. [CrossRef]

11. Kojima, K.; Tsujimoto, T.; Fujii, H.; Morimoto, T.; Yoshioka, S.; Kato, S.; Yasuhara, Y.; Aizawa, S.; Sawai, M.; Makutani, S.; et al. Pneumatosis cystoides intestinalis induced by the alpha-glucosidase inhibitor miglitol. *IM* **2010**, *49*, 1545–1548. [CrossRef] [PubMed]

12. Manna, L.; Reale, S.; Vitale, F.; Picillo, E.; Pavone, L.M.; Gravino, A.E. Real-time PCR assay in Leishmania-infected dogs treated with meglumine antimoniate and allopurinol. *Vet. J.* **2008**, *177*, 279–282. [CrossRef] [PubMed]

13. Elshahawi, S.I.; Shaaban, K.A.; Kharel, M.K.; Thorson, J.S. A comprehensive review of glycosylated bacterial natural products. *Chem. Soc. Rev.* **2015**, *44*, 7591–7697. [CrossRef] [PubMed]

14. Huang, G.; Lv, M.; Hu, J.; Huang, K.; Xu, H. Glycosylation and activities of natural products. *Mini Rev. Med. Chem.* **2016**, *16*, 1013–1016. [CrossRef] [PubMed]

15. Malmierca, M.G.; González-Montes, L.; Pérez-Victoria, I.; Sialer, C.; Braña, A.F.; García Salcedo, R.; Martín, J.; Reyes, F.; Méndez, C.; Olano, C.; et al. Searching for glycosylated natural products in actinomycetes and identification of novel macrolactams and angucyclines. *Front. Microbiol.* **2018**, *9*, 39. [CrossRef] [PubMed]

16. Pandey, R.P.; Parajuli, P.; Sohng, J.K. Metabolic engineering of glycosylated polyketide biosynthesis. *Emerg. Top. Life Sci.* **2018**, *2*, 389–403. [CrossRef]

17. Mishra, S.; Upadhaya, K.; Mishra, K.B.; Shukla, A.K.; Tripathi, R.P.; Tiwari, V.K. Carbohydrate-Based Therapeutics: A Frontier in Drug Discovery and Development. *Stud. Nat. Prod. Chem.* **2016**, *49*, 307–361.

18. Viuff, A.H.; Besenbacher, L.M.; Kamori, A.; Jensen, M.T.; Kilian, M.; Kato, A.; Jensen, H.H. Stable analogues of nojirimycin–synthesis and biological evaluation of nojiristegine and manno-nojiristegine. *Org. Biomol. Chem.* **2015**, *13*, 9637–9658. [CrossRef]

19. Schnell, O.; Weng, J.; Sheu, W.H.H.; Watada, H.; Kalra, S.; Soegondo, S.; Yamamoto, N.; Rathod, R.; Zhang, C.; Grzeszczak, W. Acarbose reduces body weight irrespective of glycemic control in patients with diabetes: Results of a worldwide, non-interventional, observational study data pool. *J. Diabetes Complicat.* **2016**, *30*, 628–637. [CrossRef]

20. DiNicolantonio, J.J.; Bhutani, J.; O'Keefe, J.H. Acarbose: Safe and effective for lowering postprandial hyperglycaemia and improving cardiovascular outcomes. *Open Heart* **2015**, *2*. [CrossRef]

21. Mahajan, G.B.; Balachandran, L. Antibacterial agents from actinomycetes-a review. *Front. Biosci.* **2012**, *4*, 240–253. [CrossRef]

22. Ishii, H.; Hirai, K.; Sugiyama, K.; Nakatani, E.; Kimura, M.; Itoh, K. Validation of a Nomogram for Achieving Target Trough Concentration of Vancomycin: Accuracy in Patients With Augmented Renal Function. *Ther. Drug Monit.* **2018**, *40*, 693–698. [CrossRef] [PubMed]

23. Torres-Giner, S.; Martinez-Abad, A.; Gimeno-Alcañiz, J.V.; Ocio, M.J.; Lagaron, J.M. Controlled delivery of gentamicin antibiotic from bioactive electrospun polylactide-based ultrathin fibers. *Adv. Eng. Mater.* **2012**, *14*, B112–B122. [CrossRef]

24. Lopez-Lazaro, M. Digoxin, HIF-1, and cancer. *Proc. Natl. Acad. Sci. USA* **2009**, *106*, E26–E26. [CrossRef] [PubMed]

25. Yonezawa, T.; Mase, N.; Sasaki, H.; Teruya, T.; Hasegawa, S.I.; Cha, B.Y.; Yagasaki, K.; Suenaga, K.; Nagai, K.; Woo, J.T. Biselyngbyaside, isolated from marine cyanobacteria, inhibits osteoclastogenesis and induces apoptosis in mature osteoclasts. *J. Cell. Biochem.* **2012**, *113*, 440–448. [CrossRef] [PubMed]

26. Neuhof, T.; Schmieder, P.; Preussel, K.; Dieckmann, R.; Pham, H.; Bartl, F.; von Döhren, H.; Hassallidin, A. A glycosylated lipopeptide with antifungal activity from the cyanobacterium Hassallia sp. *J. Nat. Prod* **2005**, *68*, 695–700. [CrossRef] [PubMed]

27. Neuhof, T.; Schmieder, P.; Seibold, M.; Preussel, K.; von Döhren, H. Hassallidin B-Second antifungal member of the Hassallidin family. *Bioorg. Med. Chem. Lett.* **2006**, *16*, 4220–4222. [CrossRef] [PubMed]

28. Perez-Zuniga, F.J.; Seco, E.M.; Cuesta, T.; Degenhardt, F.; Rohr, J.; Vallin, C.; Iznaga, Y.; Perez, M.E.; Gonzalez, L.; Malpartida, F. CE-108, a new macrolide tetraene antibiotic. *J. Antibiot.* **2004**, *57*, 197–204.

29. Lachaud, L.; Bourgeois, N.; Plourd, M.; Leproho, P.; Bastien, P.; Ouellette, M. Parasite susceptibility to amphotericin B in failures of treatment for visceral leishmaniasis in patients coinfected with HIV type 1 and Leishmania infantum. *Clin. Infect. Dis.* **2009**, *48*, e16–e22. [CrossRef]

30. Singh, N.; Kumar, M.; Singh, R.K. Leishmaniasis: Current status of available drugs and new potential drug targets. *Asian Pac. J. Trop. Med.* **2012**, *5*, 485–497. [CrossRef]

31. Fernández, M.M.; Malchiodi, E.L.; Algranati, I.D. Differential effects of paromomycin on ribosomes of Leishmania mexicana and mammalian cells. *Antimicrob. Agents Chemother.* **2011**, *55*, 86–93. [CrossRef] [PubMed]

32. Fosso, M.Y.; Li, Y.; Garneau-Tsodikova, S. New trends in the use of aminoglycosides. *MedChemComm* **2014**, *5*, 1075–1091. [CrossRef] [PubMed]

33. Kim, M.; Li, Y.X.; Dewapriya, P.; Ryu, B.; Kim, S.K. Floridoside suppresses pro-inflammatory responses by blocking MAPK signaling in activated microglia. *BMB Rep.* **2013**, *46*, 398. [CrossRef] [PubMed]

34. Lloyd, D.H.; Viac, J.; Werling, D.; Rème, C.A.; Gatto, H. Role of sugars in surface microbe–host interactions and immune reaction modulation. *Vet. Dermatol.* **2007**, *18*, 197–204. [CrossRef] [PubMed]

35. Flannery, A.; Gerlach, J.; Joshi, L.; Kilcoyne, M. Assessing bacterial interactions using carbohydrate-based microarrays. *Microarrays* **2015**, *4*, 690–713. [CrossRef] [PubMed]

36. Trouvelot, S.; Héloir, M.C.; Poinssot, B.; Gauthier, A.; Paris, F.; Guillier, C.; Combier, M.; Trdá, L.; Daire, X.; Adrian, M. Carbohydrates in plant immunity and plant protection: Roles and potential application as foliar sprays. *Front. Plant Sci.* **2014**, *5*, 592. [CrossRef]

37. Vasconcelos, A.; Pomin, V. Marine carbohydrate-based compounds with medicinal properties. *Mar. Drugs* **2018**, *16*, 233. [CrossRef]

38. Clark, G.F. The role of carbohydrate recognition during human sperm–egg binding. *Hum. Reprod.* **2013**, *28*, 566–577. [CrossRef]

39. Wang, W.; Song, X.; Wang, L.; Song, L. Pathogen-derived carbohydrate recognition in molluscs immune defense. *Int. J. Mol. Sci.* **2018**, *19*, 721. [CrossRef]

40. Feinberg, H.; Jégouzo, S.A.; Rowntree, T.J.; Guan, Y.; Brash, M.A.; Taylor, M.E.; Weis, W.I.; Drickamer, K. Mechanism for recognition of an unusual mycobacterial glycolipid by the macrophage receptor mincle. *J. Biol. Chem.* **2013**, *288*, 28457–28465. [CrossRef]

41. Glavey, S.V.; Huynh, D.; Reagan, M.R.; Manier, S.; Moschetta, M.; Kawano, Y.; Roccaro, A.M.; Ghobrial, I.M.; Joshi, L.; O'Dwyer, M.E. The cancer glycome: Carbohydrates as mediators of metastasis. *Blood Rev.* **2015**, *29*, 269–279. [CrossRef] [PubMed]

42. Camas, M.; Camas, A.S.; Kyeremeh, K. Extracellular Synthesis and Characterization of Gold Nanoparticles Using Mycobacterium sp. BRS2A-AR2 Isolated from the Aerial Roots of the Ghanaian Mangrove Plant, Rhizophora racemosa. *Indian J. Microbiol.* **2018**, *58*, 214–221. [CrossRef] [PubMed]

43. Tomlinson, P.B. *The Botany of Mangroves*, 2nd ed.; Cambridge University Press: Cambridge, UK, 1994; pp. 326–336.

44. Hughes, R.H. *A Directory of African Wetlands*; International Union of Conservation of Nature (IUCN): Gland, Switzerland; Cambridge, UK, 1992; pp. 508–510.

45. Duke, N.C.; Allen, J.A. *Atlantic–East Pacific Red Mangroves: Rhizophora Mangle, R. Samoensis, R. Racemosa, R. X Harrisonii*; Permanent Agriculture Resources (PAR): Holualoa, HI, USA, 2006; pp. 1–18.

46. Beatriz, B.M.; Barreto, E. First report of Rhizophora racemosa Meyer (Rhizophoraceae) in the mangrove forests of the Venezuelan Caribbean coast. *Interciencia* **2012**, *37*, 133–137.

47. Levasseur, A.; Asmar, S.; Robert, C.; Drancourt, M. Draft genome sequence of Mycobacterium houstonense strain ATCC 49403T. *Genome Announc.* **2016**, *4*. [CrossRef]

48. Hennessee, C.T.; Seo, J.S.; Alvarez, A.M.; Li, Q.X. Polycyclic aromatic hydrocarbon-degrading species isolated from Hawaiian soils: *Mycobacterium crocinum* sp. nov., *Mycobacterium pallens* sp. nov., *Mycobacterium rutilum* sp. nov., *Mycobacterium rufum* sp. nov. and *Mycobacterium aromaticivorans* sp. nov. *Int. J. Syst. Evol. Microbiol.* **2009**, *59*, 378–387. [CrossRef] [PubMed]

49. Hamid, M.E. Epidemiology, pathology, immunology and diagnosis of bovine farcy: A review. *Prev. Vet. Med.* **2012**, *105*, 1–9. [CrossRef]

50. McGettrick, A.F.; Corcoran, S.E.; Barry, P.J.; McFarland, J.; Crès, C.; Curtis, A.M.; Franklin, E.; Corr, S.C.; Mok, K.H.; Cummins, E.P.; et al. Trypanosoma brucei metabolite indolepyruvate decreases HIF-1α and glycolysis in macrophages as a mechanism of innate immune evasion. *Proc. Natl. Acad. Sci. USA* **2016**, *113*, E7778–E7787. [CrossRef]

51. Marchese, L.; Nascimento, J.; Damasceno, F.; Bringaud, F.; Michels, P.; Silber, A. The uptake and metabolism of amino acids, and their unique role in the biology of pathogenic trypanosomatids. *Pathogens* **2018**, *7*, 36. [CrossRef]

52. Kupchan, S.M.; Britton, R.W.; Ziegler, M.F.; Sigel, C.W. Bruceantin, a new potent antileukemic simaroubolide from Brucea antidysenterica. *J. Org. Chem.* **1973**, *38*, 178–179. [CrossRef]

53. Yabu, Y.; Minagawa, N.; Kita, K.; Nagai, K.; Honma, M.; Sakajo, S.; Koide, T.; Ohta, N.; Yoshimoto, A. Oral and intraperitoneal treatment of Trypanosoma brucei brucei with a combination of ascofuranone and glycerol in mice. *Parasitol. Int.* **1998**, *47*, 131–137. [CrossRef]